

Design of Reconfigurable Patch Antenna in Frequency, Pattern, and Switchable Polarization

Yan Zhang¹, Da Sun¹, Tao Dong², and Jie Yin²

¹ School of Electronic and Information Engineering
Beihang University, Beijing, 100191, China
yanzhang@buaa.edu.cn, sunda_buaa@163.com

² State Key Laboratory of Space-Ground Integrated Information Technology
Beijing Institute of Satellite Information Engineering, Beijing, 100095, China
dongtaoandy@163.com, kingjack333333@126.com

Abstract — In this paper, a circularly polarized frequency, pattern, and polarization switching antenna is proposed. The antenna consists of an octagonal patch, a narrow octagonal ring and four diamond-shaped parasitic patches on the top layer. Two feed points of the radiating patch are connected to a Wilkinson power divider loaded with the phase reconfigurable transmission lines on the bottom layer. Reconfiguration of the polarization and pattern is realized by using PIN diodes as switching components. By controlling the bias voltage across the varactors, various narrow frequency bands can be achieved. The proposed antenna operates at a frequency tuning range from 1.96 to 2.03 GHz. The radiation pattern can be switched among five cases in yoz-plane and xoz-plane, with the switchable polarization between left- and right-hand circular polarization. In addition, these three types of reconfiguration can be controlled independently.

Index Terms — Beam switching, frequency reconfigurable, patch antenna, switchable polarization.

I. INTRODUCTION

With the rapid development of modern wireless communication, people have a strong demand for the higher speed and quality of information transmission. Thus, antennas in modern applications must be multifunctional and adaptable with the system requirements in the varying electromagnetic environment. Reconfigurable antennas, also known as the tunable antenna, have attracted much attention.

Frequency reconfigurable antennas are realized by using PIN diodes [1-3], varactors [4-6] and MEMS [7] as the RF switches to change the size of the radiating patch or using liquid crystal [8] and metasurface [9]. Polarization reconfigurable antennas can be achieved by controlling the states of the PIN diodes to change the

structure of the feeding network [10,11] and adjust the radiation structure of the antenna [12,13]. Pattern reconfiguration or beam scanning based on PIN diodes, parasitic stubs and metamaterial structure are introduced in [14-16]. In the recent years, some efforts have been done to realize arbitrary combination of two of three reconfigurable characteristics, including frequency and polarization reconfigurable antenna [17], pattern and polarization reconfigurable antenna [18] and so on. Furthermore, some antennas with frequency, pattern reconfiguration and polarization switching have been also reported in [19,20]. However, most of reconfigurable antennas combined two or three types of reconfiguration are unable to control the antenna parameters independently.

Therefore, a novel reconfigurable patch antenna is designed to achieve three types of reconfiguration independently in this paper. By controlling the bias voltage across the varactors and PIN diodes, the three types of reconfiguration can be realized, and characteristic parameters of the antenna can be controlled independently.

II. ANTENNA DESIGN

The geometry of the proposed reconfigurable antenna is shown in Fig. 1. On the top layer of the upper substrate, an octagonal patch, as shown in Fig. 1 (a), is located at the center and surrounded by four diamond-shaped parasitic patch elements. The center radiating patch with a cross-shaped slot is fed by the Wilkinson power divider with the phase reconfigurable transmission lines.

In order to realize the frequency reconfiguration, eight varactors (D1 to D8) are located between the octagonal patch and octagonal ring. In addition, four PIN diodes are placed across the slot of parasitic patch for pattern reconfiguration. On the bottom layer of the lower

substrate, the feed network, as shown in Fig. 1 (c), consists of a Wilkinson power divider and the phase reconfigurable transmission lines with six PIN diodes (S11, S12, S21, S22, S31 and S32) providing the required phase shift along two output branch lines for different polarizations.

Two pieces of substrates with the dielectric constant ϵ_r (2.9), have a thickness of h_1 (4.5 mm) and h_2 (1.5 mm), as shown in Fig. 1 (b). The ground plane is located on the top layer of the lower substrate. And the output ports of the feed network (Port 1 and 2) are connected to the octagonal radiating patch via two probes. Detailed dimensions of the proposed antenna are listed in Table 1.

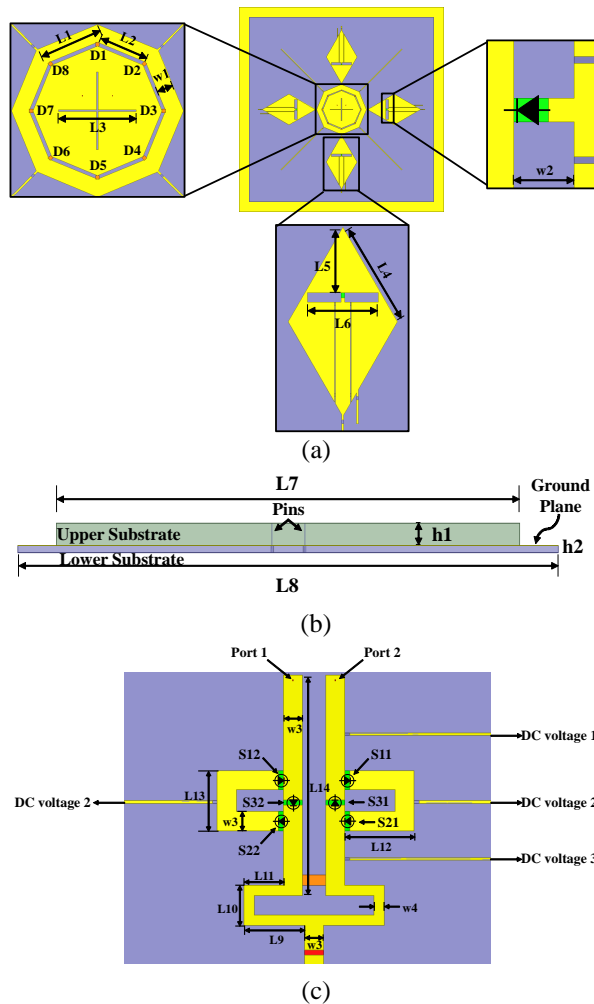


Fig. 1. Geometry of the proposed antenna: (a) top view, (b) side view, and (c) bottom view.

Table 1: Dimensions of the proposed antenna

Parameter	Value/mm	Parameter	Value/mm
L1	18.7	L11	7.9
L2	14.8	L12	13.2
L3	22	L13	12
L4	30	L14	44.1
L5	17.9	w1	5
L6	19.5	w2	2.6
L7	160	w3	3.8
L8	180	w4	2.1
L9	12.1	h1	4.5
L10	8.1	h2	1.5

III. SIMULATION AND ANALYSIS

In this section, the reconfiguration mechanism of the antenna is described in detail and the performance of the proposed antenna is simulated by using HFSS.

A. Frequency reconfiguration

The frequency reconfiguration is achieved by controlling the reverse bias voltage of the varactors, MA2S372, (D1 to D8 shown in Fig. 1 (a)) connected between the radiating patch and the octagonal ring. Under different capacitance values, the radiating patch with an octagonal ring provides several frequency bands. The equivalent capacitance of varactors at different bias voltages are listed in Table 2.

Table 2: Capacitance values of the varactor

Bias Voltage/V	Equivalent Capacitance/pF
4.5	10
6	8
9	6
13.5	4
30	2

Figure 2 shows the simulated results at different reverse bias voltages for RHCP. As the reverse bias voltage increases from 4.5 to 30 V, the resonant frequency of antenna shifts from 1.96 to 2.03 GHz, as shown in Fig. 2 (a). From Figs. 2 (b)-(c), the antenna gain is higher than 7.68 dBi and the axial ratio is below 3 dB at resonant frequency for different reverse bias voltages, which indicates good circular polarization (CP) performance during frequency reconfiguration.

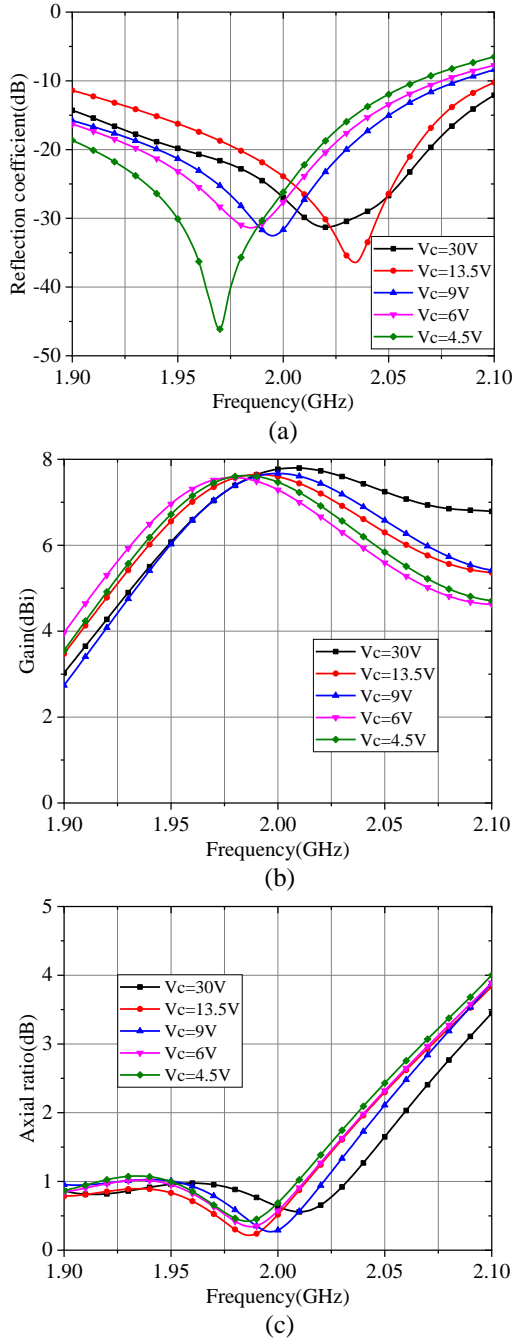


Fig. 2. Simulated results at different reverse bias voltage for RHCP: (a) reflection coefficient, (b) realized gain, and (c) axial ratio.

B. Polarization reconfiguration

The polarization reconfiguration of antenna can be realized by the Wilkinson power divider and phase reconfigurable transmission lines. By controlling the ON/OFF state of the PIN diodes, the left-hand (LH) and right-hand circular polarization (RHCP) of antenna can be chosen.

By controlling the DC voltage 1, 2 and 3 ($V_1 < V_2 < V_3$), the diodes S12, S22, S31 are in ON state, and all the other diodes are OFF. In this case, a 90° -delay transmission line is inserted into the left branch and LHCP is realized. The transmission path of the signal and the simulated radiation patterns are shown in Figs. 3 and 4.

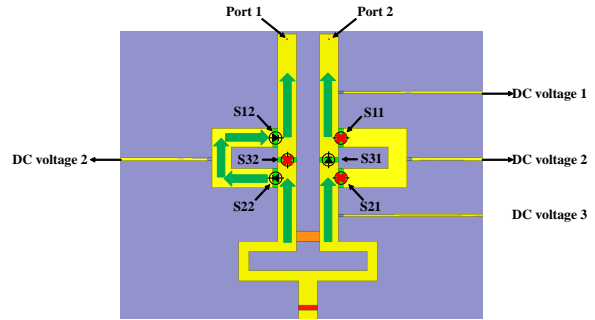


Fig. 3. Transmission path of the signal at $V_1 < V_2 < V_3$.

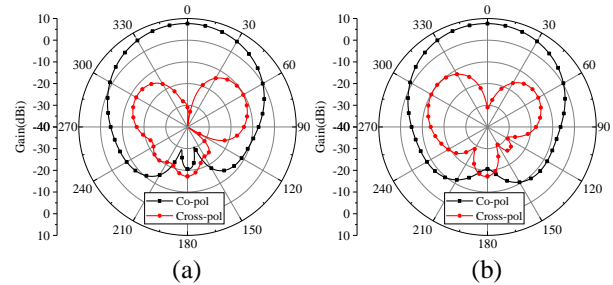


Fig. 4. Simulated LHCP radiation patterns of the antenna at 2 GHz: (a) yoz-plane and (b) xoz-plane.

It can be seen from Fig. 4 that the antenna gain is 7.68 dBi and the cross-polarization level is less than -20 dB for LHCP state.

Similarly, as the diodes S11, S21, S32 are in ON state ($V_1 > V_2 > V_3$) and all the other diodes are switched OFF, the transmission path of the signal is shown in Fig. 5. At this time, the antenna establishes the RHCP. The simulated results are shown in Fig. 6.

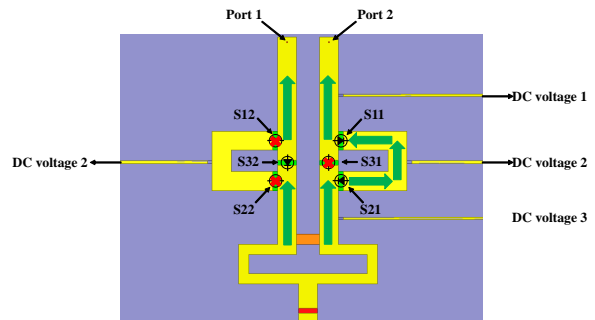


Fig. 5. Transmission path of the signal at $V_1 > V_2 > V_3$.

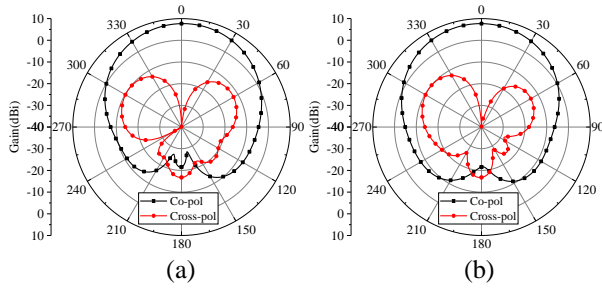


Fig. 6. Simulated RHCP radiation patterns of the antenna at 2 GHz: (a) yoz-plane and (b) xoz-plane.

From Fig. 6, the antenna gain is 7.66 dBi with the cross-polarization less than -20 dB for RHCP state. In addition, the axial ratio (AR) versus frequency of the proposed antenna for LHCP and RHCP cases is also presented in Fig. 7.

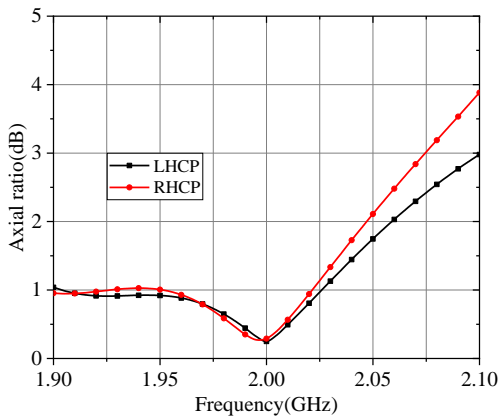


Fig. 7. Simulated axial ratio of the proposed antenna in two CP states for LHCP and RHCP.

It can be seen from Fig. 7 that the AR is 0.3 dB at 2 GHz. Compared with Figs. 2 (a) and (c), good CP performance ($AR < 1$ dB) can be observed in the whole of reconfigure frequency range from 1.96 to 2.03 GHz.

C. Pattern reconfiguration

The pattern reconfiguration is achieved by changing the OFF/ON state of the PIN diodes (S1 to S4) on the parasitic patch A, B, C and D, as shown in Fig. 8.

The surface current distributions for the radiating and parasitic patches for three cases are shown in Fig. 9.

As S1-S4 are in ON state, the surface current is mainly located at the radiating patch, as shown in Fig. 9 (a). As S1 is in OFF state, the surface current on the parasitic patch A, where S1 is located, increased significantly, as shown in Fig. 9 (b). And the main beam tilts toward +y direction. Similarly, the main beam tilts toward -y direction as S2 is in OFF state, as shown in

Fig. 9 (c). The information on the state of four PIN diodes for five cases is listed in Table 3.

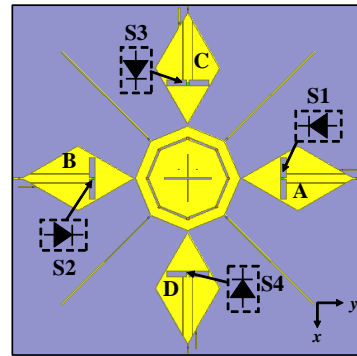


Fig. 8. Structure of the pattern reconfiguration module.

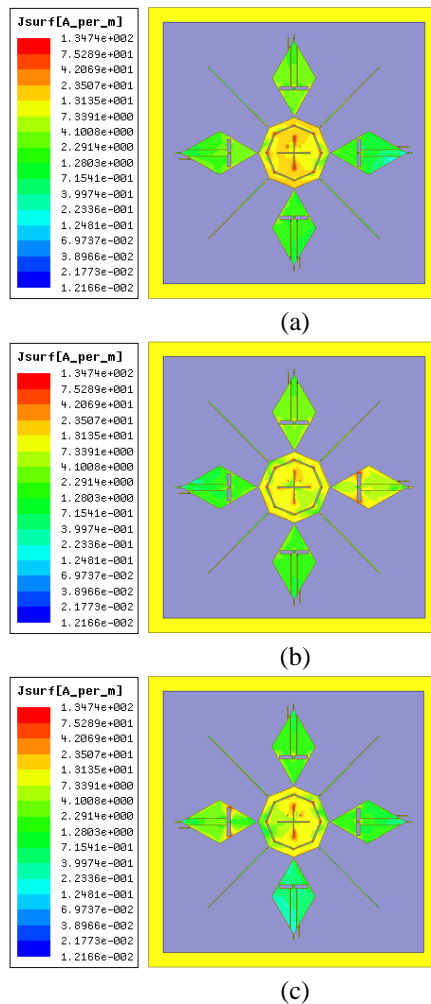


Fig. 9. Simulated surface current distributions at 2 GHz in different cases: (a) S1-S4 are ON, (b) S1 is OFF, and others are ON, (c) S2 is OFF, and others are ON.

Table 3: The state of four PIN diodes for five cases

Case	S1	S2	S3	S4	Pattern Mode
1	ON	ON	ON	ON	Boresight
2	OFF	ON	ON	ON	+y-direction tilted
3	ON	OFF	ON	ON	-y-direction tilted
4	ON	ON	OFF	ON	-x-direction tilted
5	ON	ON	ON	OFF	+x-direction tilted

Taking the polarization state of RHCP as an example, when the bias voltage across the varactor D1 to D8 is 9V, the resonance frequency of the antenna is 2GHz. In order to evaluate the impedance characteristics of antenna for these four pattern reconfiguration cases, the simulated reflection coefficients are provided in Fig. 10.

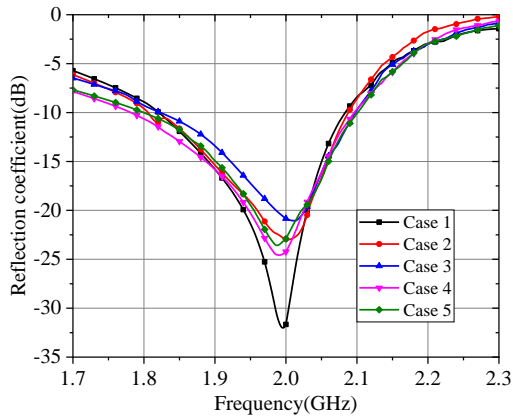


Fig. 10. Simulated reflection coefficient for five cases ($V_c=9V$).

It is noticed from Fig. 10 that the antenna operates in the frequency band of 1.82-2.09 GHz with reflection coefficient of less than -10 dB for different cases. Detailed information on simulation results is listed in Table 4.

Table 4: Impedance characteristics for five cases

Case	Center Frequency/ GHz	Bandwidth/ %	-10dB Band Range/GHz
1	1.96	13.8	1.82~2.09
2	1.95	14.4	1.81~2.09
3	1.96	14.3	1.82~2.10
4	1.94	15.5	1.79~2.09
5	1.95	15.4	1.80~2.10

The simulated radiation efficiency of the proposed antenna for five cases is shown in Fig. 11.

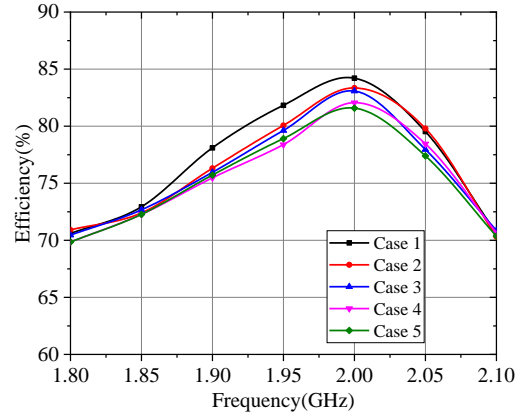


Fig. 11. Simulated radiation efficiency of the proposed antenna in different cases for $V_c=9V$.

From Fig. 11, results of the simulation indicate that the proposed antenna features a good efficiency, being greater than 70% in the whole operating frequency range for five cases. Meanwhile, the simulated RHCP radiation patterns at 2GHz for five cases are shown in Fig. 12.

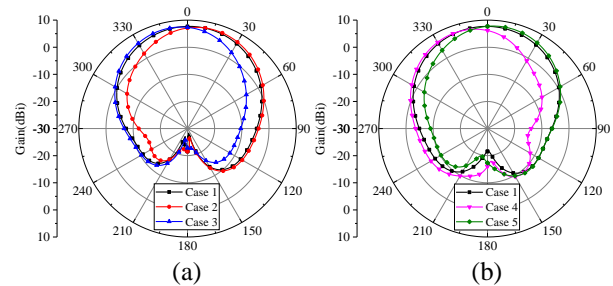


Fig. 12. Simulated RHCP radiation patterns of the antenna for five cases at 2 GHz: (a) yoz-plane and (b) xoz-plane.

It can be seen from Fig. 12 that: 1) the main beam could tilt toward five directions for pattern reconfiguration; 2) the beamwidth becomes narrower as the main beam tilts.

For the comparison purpose, the simulated LHCP radiation patterns at 2 GHz for five cases are also shown in Fig. 13. And detailed simulation results of radiation characteristics are listed in Table 5 and 6.

It can be seen from Table 5 and 6, for LHCP in Case 1, the main beam direction is at -1° in yoz-plane with a 3dB beamwidth from -40.6° to 37° . Therefore, the main beam direction of the proposed antenna can be pointed to approximate 10° and -10° in yoz-plane for Case 2 and Case 3, respectively, with the realized gain around 7.62-7.64 dBi. Similarly, when the diodes operate in Case 4 and Case 5, the main beam of the pattern can be pointed to -15° and 10° in xoz-plane with the realized gain around 7.27-7.84 dBi. In addition, when the antenna operates in

RHCP, the main beam direction of the proposed antenna can be pointed to approximate 1° , 13° , -13° in yoz-plane and -17° , 10° in xoz-plane for Case 1 to Case 5. The difference of the radiation patterns in yoz-plane and xoz-plane is mainly due to the asymmetry of the feed network.

The peak gain and axial ratio at the main beam for five cases are presented in Fig. 14.

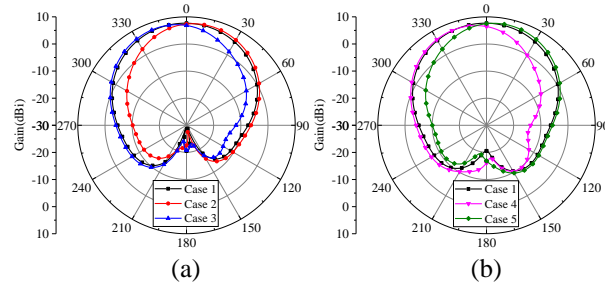


Fig. 13. Simulated LHCP radiation patterns of the antenna for five cases at 2 GHz: (a) yoz-plane and (b) xoz-plane.

Table 5: Radiation characteristics of the proposed antenna in yoz-plane

Case	Polarization	Gain/dBi	Beam Direction	3dB Beam Range
1	LHCP	7.67	-1°	$-40.6^\circ \sim 37^\circ$
	RHCP	7.70	1°	$-40.5^\circ \sim 36^\circ$
2	LHCP	7.64	10°	$-19.8^\circ \sim 42^\circ$
	RHCP	7.68	13°	$-16.5^\circ \sim 46^\circ$
3	LHCP	7.62	-10°	$-41.3^\circ \sim 20^\circ$
	RHCP	7.53	-13°	$-46.3^\circ \sim 15^\circ$

Table 6: Radiation characteristics of the proposed antenna in xoz-plane

Case	Polarization	Gain/dBi	Beam Direction	3dB Beam Range
1	LHCP	7.66	0°	$-40.7^\circ \sim 37^\circ$
	RHCP	7.68	0°	$-41.0^\circ \sim 37^\circ$
4	LHCP	7.27	-15°	$-46.7^\circ \sim 13^\circ$
	RHCP	7.09	-17°	$-48.7^\circ \sim 10^\circ$
5	LHCP	7.84	10°	$-18.8^\circ \sim 42^\circ$
	RHCP	7.95	10°	$-21.7^\circ \sim 41^\circ$

From Fig. 14 (a), it can be observed that the peak gain in yoz-plane is about 7.68 dBi with 0.05 dB and 0.17 dB variation along the beam direction for LHCP and RHCP, respectively. In Fig. 14 (b), the peak gain at 0° has a variation of 0.39 dB and 0.59 dB along the beam direction in xoz-plane for LHCP and RHCP. In addition, the axial ratio along the main beam direction for five cases is less than 3dB for CP reconfiguration.

In order to demonstrate that the radiation pattern of the antenna in CP state can be switched among five cases

within the frequency reconfigurable range from 1.96 to 2.03 GHz, the simulated results are provided in Fig. 15 and Fig. 16.

Figure 15 and Fig. 16 present the co-polarization and cross-polarization radiation patterns for RHCP in different cases at 1.96 GHz ($V_c=4.5V$) and 2.03GHz ($V_c=30V$), respectively.

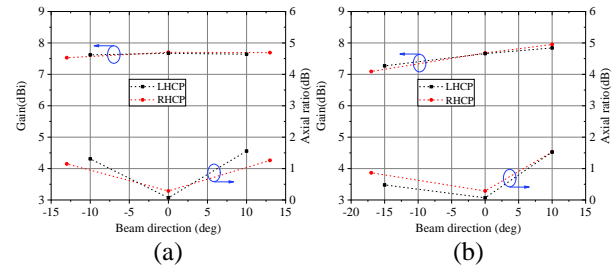


Fig. 14. Simulated peak gain and axial ratio versus the beam direction angles at 2 GHz: (a) yoz-plane and (b) xoz-plane.

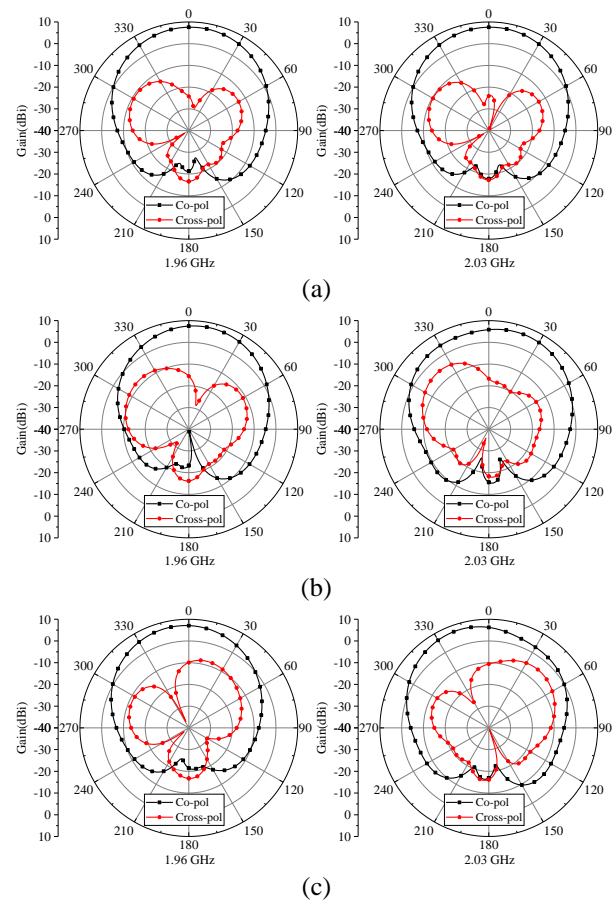


Fig. 15. Simulated RHCP radiation patterns in yoz-plane at 1.96 GHz and 2.03 GHz: (a) Case 1, (b) Case 2, and (c) Case 3.

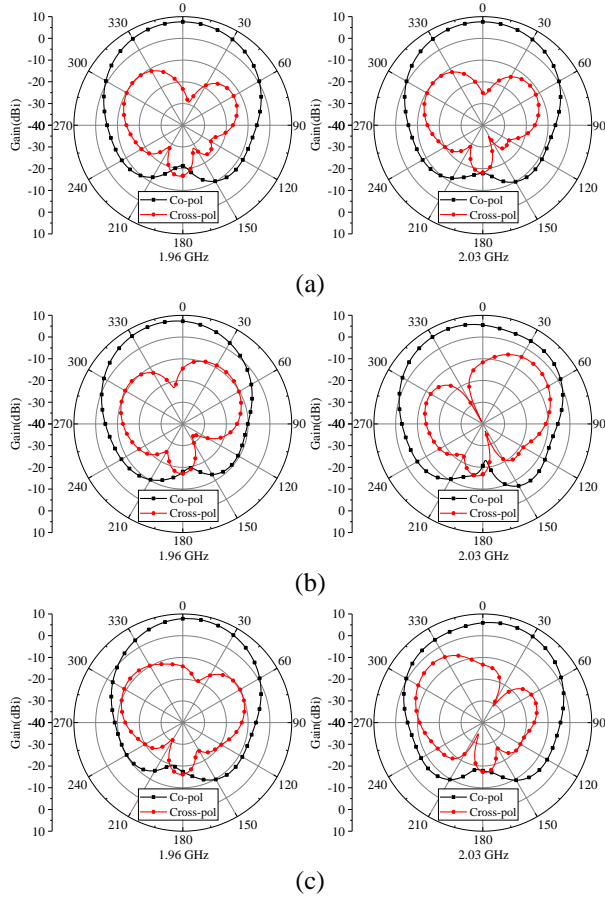


Fig. 16. Simulated RHCP radiation patterns in xoz-plane at 1.96 GHz and 2.03 GHz: (a) Case 1, (b) Case 4, and (c) Case 5.

The main beam direction of the pattern can be pointed to approximate 0° , 10° , -6° in yoz-plane and -1° , -10° , 7° in xoz-plane with cross-polarization levels less than -15 dB at 1.96 GHz. Similarly, when the antenna operates at 2.03 GHz, the beam direction can be pointed to approximate 3° , 17° , -16° in yoz-plane and -1° , -19° , 14° in xoz-plane with cross-polarization levels less than -10 dB. All the above simulated results indicate that the proposed antenna can realize pattern reconfiguration in LHCP and RHCP during the reconfigure frequency range.

IV. MEASUREMENT RESULTS AND DISCUSSION

An antenna prototype is fabricated and tested for impedance and radiation characteristics of the proposed design. A photo of the fabricated antenna prototype is shown in Fig. 17.

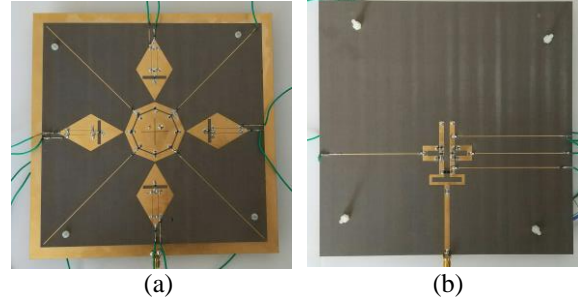


Fig. 17. Photographs of the proposed antenna: (a) top view and (b) bottom view.

The measured reflection coefficient of the antenna is presented in Fig. 18.

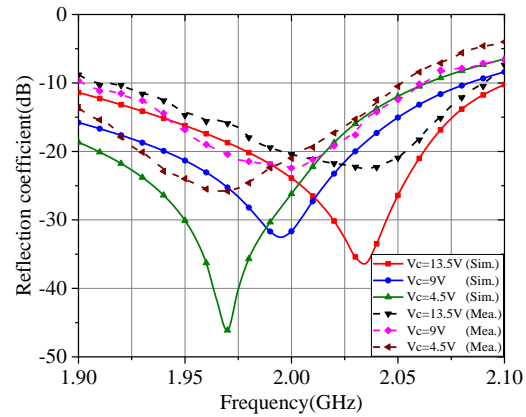


Fig. 18. Simulated and measured reflection coefficient at different reverse bias voltage.

From Fig. 18, it can be seen that the resonant frequency ranges from 1.96 to 2.03 GHz as the bias voltage increases from 4.5 to 13.5V. The differences between the measured and simulated data may be related to the mismatch caused by external connectors, the deviation of the substrate dielectric constant, and the processing error of the structure.

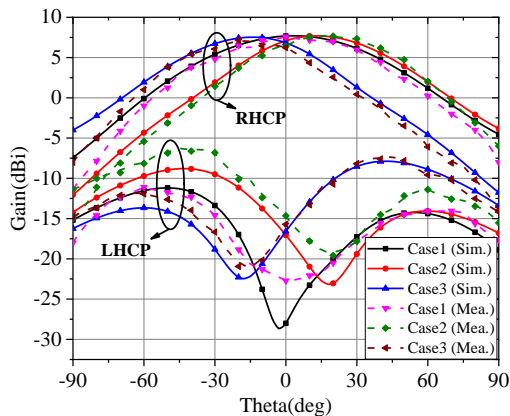
The measured radiation performance of the antenna is shown in Fig. 19.

Figure 19 shows that the agreement between the simulation results and the measured data is reasonably good.

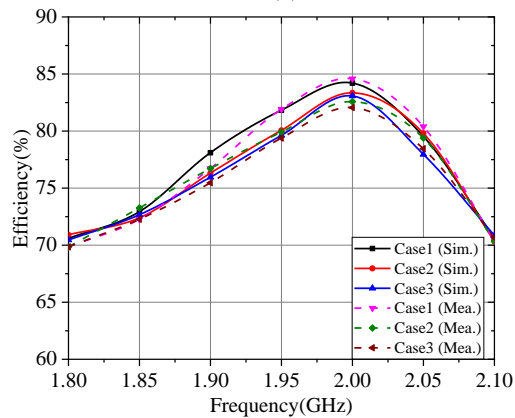
Compared with the existing designs of reconfigurable antennas listed in Table 7, the proposed work has the advantages of low profile, high efficiency, and multiple functions, which is very attractive in mobile communication.

Table 7: Compared with the reported reconfigurable antennas

Ref.	Type	Reconfiguration	Actuators	η (%)	Size (λ_0)
[21]	Patch	Frequency and polarization	12 Varactors	60	0.62×0.62×0.03
[22]	Patch	Frequency and pattern	4 PIN diodes	78	0.67×0.67×0.02
[23]	Slot	Polarization and pattern	9 PIN diodes	75	4.5×1.1×0.08
[19]	Patch and pixel layer	Frequency, polarization and pattern	60 PIN diodes	53	2.1×1.1×0.07
[20]	Slot	Frequency, polarization and pattern	48 PIN diodes	49	0.86×0.78×0.01
This work	Patch	Frequency, polarization and pattern	10 PIN diodes and 8 Varactors	70	1.2×1.2×0.04



(a)



(b)

Fig. 19. Simulated and measured RHCP results of the proposed antenna for $V_c=9V$: (a) radiation patterns in the yoz-plane (at 2 GHz), and (b) radiation efficiency.

V. CONCLUSION

A novel patch antenna design for frequency, pattern, and polarization reconfiguration has been presented in this paper. By using varactors and PIN diodes, these three kinds of characteristics of the antenna could become reconfigurable independently. Simulations about impedance and radiation characteristics of the antenna have been carried out for different cases. To validate this antenna design, a S-band patch antenna is fabricated and

measured as an example. It is found that the polarization (LHCP/RHCP), resonant frequency (1.96 to 2.03 GHz) and radiation pattern reconfiguration can be realized independently. With the multiple functions and a low-profile structure, the proposed antenna could be applied to mobile communication, satellites communication and telemetry systems. Besides, it can also improve signal-to-noise ratio and increase the spectrum utilization of the wireless communication by dynamically adjusting frequency, polarization or radiation characteristics. In the future, methods of adaptive adjustment will be further investigated to better meet the communication needs in different scenarios.

ACKNOWLEDGMENT

This work was supported in part by the CAST Innovation Fund (China Academy of Space Technology), in part by the Aerospace Science and Technology Innovation Fund (China Aerospace Science and Technology Corporation), in part by the Open Research Fund of State Key Laboratory of Space-Ground Integrated Information Technology under grant NO. 2015_SGIIT_KFJJ_TX_01.

REFERENCES

- [1] M. Shirazi, J. Huang, T. Li, and X. Gong, "A switchable-frequency slot-ring antenna element for designing a reconfigurable array," *IEEE Antennas and Wireless Propag. Lett.*, vol. 17, no. 2, pp. 229-233, Feb. 2018.
- [2] L. Pazin and Y. Leviatan, "Reconfigurable slot antenna for switchable multiband operation in a wide frequency range," *IEEE Antennas and Wireless Propag. Lett.*, vol. 12, pp. 329-332, 2013.
- [3] T. Li, H. Zhai, X. Wang, L. Li, and C. Liang, "Frequency-reconfigurable bow-tie antenna for bluetooth, WiMAX, and WLAN applications," *IEEE Antennas and Wireless Propag. Lett.*, vol. 14, pp. 171-174, 2015.
- [4] B. Babakhani and S. Sharma, "Wideband frequency tunable concentric circular microstrip patch antenna with simultaneous polarization reconfiguration," *IEEE Antennas and Propagation Magazine*, vol. 57,

- no. 2, pp. 203-216, Apr. 2015.
- [5] S. Honda, S. Saito, and Y. Kimura, "Frequency control of a varactor-loaded dual-band single-layer shorted multi-ring microstrip antenna fed by an L-probe with reduced patch area in half," *2019 International Symposium on Antennas and Propagation (ISAP)*, pp. 1-3, 2019.
- [6] M. W. Young, S. Yong, and J. T. Bernhard, "A miniaturized frequency reconfigurable antenna with single bias, dual varactor tuning," *IEEE Trans. Antennas Propag.*, vol. 63, no. 3, pp. 946-951, Mar. 2015.
- [7] A. Zohur, H. Mopidevi, D. Rodrigo, M. Unlu, L. Jofre, and B. A. Cetiner, "RF MEMS reconfigurable two-band antenna," *IEEE Antennas and Wireless Propag. Lett.*, vol. 12, pp. 72-75, 2013.
- [8] Y. Zhao, C. Huang, A. Qing, and X. Luo, "A frequency and pattern reconfigurable antenna array based on liquid crystal technology," *IEEE Photonics Journal*, vol. 9, no. 3, pp. 1-7, June 2017.
- [9] B. Majumder, K. Krishnamoorthy, J. Mukherjee, and K. P. Ray, "Frequency-reconfigurable slot antenna enabled by thin anisotropic double layer metasurfaces," *IEEE Trans. Antennas Propag.*, vol. 64, no. 4, pp. 1218-1225, Apr. 2016.
- [10] S. M. Kumar and Y. K. Choukiker, "Frequency and polarization reconfigurable microstrip antenna with switching feed configuration," *2018 IEEE Indian Conference on Antennas and Propagation (InCAP)*, Hyderabad, India, pp. 1-4, 2018.
- [11] S. W. Lee and Y. J. Sung, "Simple polarization-reconfigurable antenna with T-shaped feed," *IEEE Antennas and Wireless Propag. Lett.*, vol. 15, pp. 114-117, 2016.
- [12] P. Pan and B. Guan, "A wideband polarization reconfigurable antenna with six polarization states," *2018 12th International Symposium on Antennas, Propagation and EM Theory (ISAPE)*, Hangzhou, China, pp. 1-4, 2018.
- [13] J. Row and Y. Wei, "Wideband reconfigurable crossed-dipole antenna with quad-polarization diversity," *IEEE Trans. Antennas Propag.*, vol. 66, no. 4, pp. 2090-2094, Apr. 2018.
- [14] G. Yang, J. Li, D. Wei, S. Zhou, and R. Xu, "Pattern reconfigurable microstrip antenna with multidirectional beam for wireless communication," *IEEE Trans. Antennas Propag.*, vol. 67, no. 3, pp. 1910-1915, Mar. 2019.
- [15] M. Jusoh, T. Aboufoul, T. Sabapathy, A. Alomainy, and M. R. Kamarudin, "Pattern-reconfigurable microstrip patch antenna with multidirectional beam for WiMAX application," *IEEE Antennas and Wireless Propag. Lett.*, vol. 13, pp. 860-863, 2014.
- [16] S. Yan and G. A. E. Vandenbosch, "Radiation pattern-reconfigurable wearable antenna based on metamaterial structure," *IEEE Antennas and Wireless Propag. Lett.*, vol. 15, pp. 1715-1718, 2016.
- [17] L. Tan, R. Wu, and Y. Poo, "Magnetically reconfigurable SIW antenna with tunable frequencies and polarizations," *IEEE Trans. Antennas Propag.*, vol. 63, no. 6, pp. 2772-2776, June 2015.
- [18] W. Yang, W. Che, H. Jin, W. Feng, and Q. Xue, "A polarization-reconfigurable dipole antenna using polarization rotation AMC structure," *IEEE Trans. Antennas Propag.*, vol. 63, no. 12, pp. 5305-5315, Dec. 2015.
- [19] D. Rodrigo, B. A. Cetiner, and L. Jofre, "Frequency, radiation pattern and polarization reconfigurable antenna using a parasitic pixel layer," *IEEE Trans. Antennas Propag.*, vol. 62, no. 6, pp. 3422-3427, June 2014.
- [20] L. Ge, Y. Li, J. Wang, and C. Sim, "A low-profile reconfigurable cavity-backed slot antenna with frequency, polarization, and radiation pattern agility," *IEEE Trans. Antennas Propag.*, vol. 65, no. 5, pp. 2182-2189, May 2017.
- [21] N. Nguyen-Trong, L. Hall, and C. Fumeaux, "A frequency- and polarization-reconfigurable stub-loaded microstrip patch antenna," *IEEE Trans. Antennas Propag.*, vol. 63, no. 11, pp. 5235-5240, Nov. 2015.
- [22] Y. P. Selvam, M. Kanagasabai, M. G. N. Alsath, S. Velan, S. Kingsly, S. Subbaraj, Y. V. Ramana Rao, R. Srinivasan, A. K. Varadhan, and M. Karupiah, "A low-profile frequency- and pattern-reconfigurable antenna," *IEEE Antennas and Wireless Propag. Lett.*, vol. 16, pp. 3047-3050, 2017.
- [23] S. Chen, D. K. Karmokar, P. Qin, R. W. Ziolkowski, and Y. J. Guo, "Polarization-reconfigurable leaky-wave antenna with continuous beam scanning through broadside," *IEEE Trans. Antennas Propag.*, vol. 68, no. 1, pp. 121-133, Jan. 2020.



Yan Zhang received the B.S. and Ph.D. degrees in Electromagnetic Field and Microwave Technology from the Beijing University of Aeronautics and Astronautics (BUAA), Beijing, China, in 2002 and 2006, respectively. From 2007 to 2008, he was a Post-Doctoral Researcher with the Communication, Navigation, Surveillance/Air Traffic Management (CNS/ATM) Laboratory, Civil Aviation Administration of China (CAAC), BUAA. He is currently an Associate Professor of Electronics and Information Engineering with BUAA.

He has authored over 40 papers. His research interests include antenna, electromagnetic surface and antenna array. Zhang was the recipient of the Outstanding Doctoral Dissertation Award and the Outstanding Post-Doctoral Researcher Award presented by BUAA in 2008.



Da Sun received the degree in Electronics and Information Engineering in 2018. He is currently pursuing the M.S. degree in Electronic Science and Technology, School of Electronics and Information Engineering, Beihang University, Beijing, China. His research interests include antenna, electromagnetic surface and antenna array.



Tao Dong received the B.S. and Ph.D. degrees in Electronics Science and Technology from Beijing Institute of Technology in 1999 and 2004, respectively. He is currently a Professor with State Key Laboratory of Space-Ground Integrated Information Technology, Beijing Institute of Satellite Information Engineering. His research interests include antenna, phased array and optoelectronic devices.



Jie Yin received the B.S. and Ph.D. degrees in Electronics Science and Technology from Beijing University of Posts and Telecommunications (BUPT) in 2005 and 2010, respectively. He is currently a Senior Engineer in State Key Laboratory of Space-Ground Integrated Information Technology, Beijing Institute of Satellite Information Engineering. His research interests include free space optical communication, space optical networks and microwave photonics.